Kinetics and Extent of Fusion between Sendai Virus and Erythrocyte Ghosts: Application of a Mass Action Kinetic Model†

Shlomo Nir*

Seagram Center for Soil and Water Sciences, Faculty of Agriculture, The Hebrew University of Jerusalem, Rehovot 76100, Israel

Karin Klappe and Dick Hoekstra

Laboratory of Physiological Chemistry, Unversity of Groningen, Bloemsingel 10, 9712 KZ Groningen, The Netherlands

Received September 13, 1985

ABSTRACT: The kinetics and extent of fusion between Sendai virus and erythrocyte ghosts were investigated with an assay for lipid mixing based on the relief of self-quenching of fluorescence. The results were analyzed in terms of a mass action kinetic model, which views the overall fusion reaction as a sequence of a second-order process of virus–cell adhesion followed by the first-order fusion reaction itself. The fluorescence development during the course of the fusion process was calculated by numerical integration, employing separate rate constants for the adhesion step and for the subsequent fusion reaction. Dissociation of virus particles from the cells was found to be of minor importance when fusion was initiated by mixing the particles at 37 °C. However, besides the initiation of fusion, extensive dissociation does occur after a preincubation of a concentrated suspension of particles at 4 °C followed by a transfer of the sample to 37 °C. The conclusion drawn from the levels of fluorescence increase obtained after 20 h of incubation is that in principle most virus particles can fuse with the ghosts at 37 °C and pH 7.4. However, the number of Sendai virus particles that actually fuse with a single ghost is limited to 100–200, despite the fact that more than 1000 particles can bind to one cell. This finding may imply that 100–200 specific fusion sites for Sendai virus exist on the erythrocyte membrane. A simple equation can yield predictions for the final levels of fluorescence for a wide range of ratios of virus particles to ghosts. The rate constants of adhesion were very high, close to those expected in diffusion-controlled processes. The fusion rate constants were relatively small, but the calculations indicate that 1–2 min after the onset of the interaction between virus particles and ghosts at 37 °C and pH 7.4 most of the virus particles associated with the ghost have fused, provided that the number of virus particles per cell is below 100.

Sendai virus is a membrane-enveloped virus that belongs to the family of paramyxoviruses. Imperative for survival of the virus is the ability to introduce its nucleocapsid into the cytoplasma of the host cell for replication. The entry process involves initial attachment of the virions to the cell surface and subsequent fusion between the viral envelope and the plasma membrane of the host cell (Choppin & Scheid, 1980; Poste & Pasternak, 1978; Lenard & Miller, 1983; White et al., 1983). It is well-known that binding and fusion are mediated by the viral membrane proteins HN and F, respectively, which are present as spikelike projections on the surface of the virions (Haywood, 1974; Hosaka & Shimizu, 1977; Choppin & Scheid, 1980). Cell attachment is accomplished by an interaction between HN and sialic acid containing glycoproteins (Bächi et al., 1977; Umeda et al., 1983) and/or glycolipids (Holmgren et al., 1980; Umeda et al., 1984). Fusion is critically dependent on the temperature (Bächi et al., 1977; Lee et al., 1983; Hoekstra et al., 1984a). With erythrocyte ghosts as the target membrane, optimal fusion activity is seen at approximately 37 °C while its activity is insignificant at temperatures below 23 °C. As a function of pH, virus–erythrocyte membrane fusion is most pronounced around pH 7.5–8.0 (Hoekstra et al., 1985a). The molecular details of the fusion mechanism have not been resolved yet.

Recently, we developed a membrane fusion assay based on the relief of self-quenching of fluorescence, which allows a sensitive and continuous monitoring of fusion between native biological membranes (Hoekstra et al., 1984). Using this technique, we have studied the fusion kinetics of fusion of Sendai virus (Hoekstra et al., 1985a) and reconstituted Sendai virus envelopes (Harmsen et al., 1985) with erythrocyte membranes. A detailed kinetic analysis of the fusion process may facilitate the efforts to more accurately define the distinct steps involved in fusion, i.e., the initial binding and then the fusion event per se (Wilschut and Hoekstra, 1984).

The model presented here provides the possibility to "uncouple" the kinetics of binding and fusion, respectively. The procedure has yielded primary rate constants for the aggregation and fusion process during liposome–liposome interaction, and it enables one to obtain a more detailed description and prediction of the kinetics of the overall fusion process (Nir et al., 1982, 1983; Bentz et al., 1983a,b, 1985; Wilschut et al., 1985). Recently, the model has been successfully extended to evaluate the kinetics of fusion between influenza virus and cardiolipin liposomes (Nir et al., 1986). For the first time, this theoretical methodology has now been adapted to a system involving fusion between biological membranes, such as between a virus and a cell. By simulating the kinetics of fusion between Sendai virus and erythrocyte membranes in terms of

† This work was supported by National Institutes of Health Grant GM-31506 (J. Bentz and S.N.) and EMBO (short-term fellowship to S.N.).

* Address correspondence to this author at the Laboratory of Cell Biology and Genetics, National Institutes of Health, Bethesda, MD 20205, and Uniformed Services University of the Health Sciences, Bethesda, MD 20814.

0006-2960/86/0425-2155$01.50/0

the model, we have obtained the separate rate constants for virus attachment and detachment and for the actual fusion process.

In addition, from the analysis of the final levels of fluorescence, as determined after an incubation of 20 h or more, we could also deduce that (i), in principle, all virus particles are capable of fusing with the target membrane but (ii) the number of "fusion sites" per cell is limited. We demonstrate how to determine the number of fusion sites, and the results yield that 100–200 Sendai virus particles can fuse with one erythrocyte ghost.

Experimental Procedures

Virus. Sendai virus, Z strain, was grown in embryonated eggs, purified as previously described (Hoekstra et al., 1985a), and stored at −70 °C. Virus was quantitated by protein measurement with bovine serum albumin as the standard.

Preparation of R_{18}-Labeled Virus. The fluorescent probe octadecyl Rhodamine B chloride (R_{18};[1] Molecular Probes Inc., Junction City, OR) was inserted into the viral bilayer by rapid injection, under vigorous vortexing, of an ethanolic solution of the fluorophore (15 μM) into 1 mL of 120 mM KCl/30 mM NaCl/10 mM sodium phosphate (KNP buffer), pH 7.4, containing 1.5 mg of virus protein (Hoekstra et al., 1984, 1985a). After an incubation for 1 h at room temperature, noninserted probe and aggregated viral particles were removed by gel filtration on Sephadex G-75, with KNP buffer as the elution buffer. R_{18}-labeled virus was recovered in the void volume fraction.

Erythrocyte Ghosts. Human red blood cells (type A^+) were obtained from the Red Cross Blood Bank. Ghosts were prepared by hypotonic lysis of the erythrocytes in 5 mM sodium phosphate, pH 8 at 4 °C, essentially as described by Steck and Kant (1974), with some minor modifications (Hoekstra et al., 1985b). The ghosts were loaded with albumin (5% w/v), resealed, and purified as described in detail elsewhere (Hoekstra et al., 1985b). The concentration of ghosts is expressed as micrograms of protein per 2 mL. The amount of protein was determined prior to addition of albumin by the Lowry method and, in some cases, verified by lipid phosphorus determination after lipid extraction, assuming that 1 mg of protein corresponds to 674 nmol of phospholipid (Cohen & Solomon, 1976). By cell counting, it was estimated that 1 mg of protein equals approximately 1.8×10^9 cells.

Virus–Ghost Fusion. Fusion between R_{18}-labeled virus and erythrocyte ghosts was monitored continuously by following the relief of R_{18} fluorescence self-quenching. The principle and details of this assay have been described elsewhere (Hoekstra et al., 1984, 1985a). Briefly, under the conditions of labeling as described above, R_{18} is inserted into the viral membrane at a surface density that causes self-quenching of fluorescence. At the probe concentration used, the extent of self-quenching is linearly related to the surface density of the probe. Upon fusion with the (nonlabeled) erythrocyte membrane, relief of self-quenching will occur as the surface density of R_{18} decreases. The concomitant increase in fluorescence intensity is related to the extent of fusion as described under Theory.

Fusion was initiated by adding the desired amount of ghosts to a cuvette, containing R_{18}-labeled Sendai virus, suspended in KNP buffer, pH 7.4 at 37 °C. In some experiments R_{18}-labeled virus was incubated with the ghosts on ice for 15 min to allow virus attachment prior to fusion. The final incubation volume was 100–200 μL. The suspension was subsequently mixed with prewarmed buffer and immediately transferred to a cuvette, which was then placed in the fluorometer (Perkin-Elmer MPF43). In all fusion experiments, the final incubation volume was 2 mL while the temperature was kept at 37 °C with a thermostated circulating water bath. During monitoring of R_{18} fluorescence (λ_{ex} = 560 nm, λ_{em} = 590 nm, slit width 4.5 nm), the mixture was stirred with a magnetic stirring device.

The fluorescence scale was calibrated by setting the residual fluorescence of R_{18}-labeled virus at the zero level of the chart recorder and the fluorescence obtained after addition of Triton X-100 (1% v/v), corrected for sample dilution, at 100% (infinite dilution). The final extents of fusion were determined from the level of R_{18} fluorescence reached after an incubation for 24 h at 37 °C.

Theory

Mass Action Kinetics of Erythrocyte–Ghost Fusion with Sendai Virus. The fusion process is viewed as a sequence of two composite steps: (i) adherence of virus particles to the erythrocyte ghosts and (ii) the fusion process itself, which involves membrane destabilization and membrane merging (Nir et al., 1980a, 1982, 1983; Bentz et al., 1983a,b). Deaggregation processes can also occur and are explicitly taken into account.

The procedure described here follows the same lines as in a recent study on the fusion of influenza virus with phospholipid vesicles (Nir et al., 1986). However, the differential equations and their numerical solutions are quite different. A major difference stems from the fact that many virus particles can fuse with a single ghost particle, whereas vesicle–influenza virus fusion products include one or several vesicles but only a single virus. On the other hand, the calculations were significantly simplified by ignoring fusion between ghost particles because it would have a minor effect on the kinetics of fluorescence increase. Besides, most experiments were carried out by mixing the virus and ghosts directly at 37 °C. Under such conditions ghost–ghost fusion does not occur (Hoekstra et al., 1984).

Notations. The molar concentration of an aggregation–fusion product consisting of I virus particles adhering to a ghost particle, and J virus particles which have fused with it, will be denoted by $AF(I,J)$. The molar concentration of virus particles will be denoted by V. Initially, at time $t = 0$, $V(t) = V_0$. Mass conservation of virus particles is expressed by

$$V_0 = V + \sum_{I+J=1}^{N} AF(I,J)(I + J) \qquad (1)$$

in which N is the largest number of virus particles that can be associated with a single ghost particle. The molar concentration of free ghost particles is denoted by $G = AF(0,0)$. Initially, $G(t) = G_0$. Mass conservation for the ghost particles gives

$$G_0 = \sum_{I+J=0}^{N} AF(I,J) \qquad (2)$$

In formulating and solving the set of nonlinear differential equations that describe aggregation and fusion, we have employed only three parameters: C (M^{-1} s^{-1}), the rate constant of adhesion of virus to ghost particles; f (s^{-1}), the rate constant of the actual fusion of an adhered virus particle; D (s^{-1}), the

[1] Abbreviations: R_{18}, octadecyl Rhodamine B chloride; KNP buffer, 120 mM KCl/30 mM NaCl buffered with 10 mM sodium phosphate, pH 7.4.

Table I: Final Intensity Levels of R_{18} Fluorescence: Experimental and Calculated Values

virus concn (μg of protein/2 mL)		erythrocyte ghost concn (μg of protein/2 mL)											
		20	30	40	50	60	70	90	110	120	130	150	180
11.1	exptl	23.9	37.5	48.1	53.9	63.2	64.5	77.5	79.4		80	84.9[a]	
	calcd	23.9[b]	35.7	47.6	59.5	69.2	72.4	77.1	80.5		83	84.9	
15	exptl	18	27.7	38.3	44.8	51.4	55.4	65.7		72.5		78.1	82.5
	calcd	17.7	26.5	35.4	44.2	53.1	61.9	71.3		76.8		80.5	83.2
18.5	exptl	13.8	26.4	29.7	48.3		63.7	69.1					
	calcd	14.3	21.4	28.6	35.7		50.1	64.4					

[a] Experimental value used to determine S_v/S_e (see eq 10). [b] Experimental value used to determine N (see eq 11).

deadhesion rate constant. The kinetics of adhesion, deadhesion, and fusion is described by the equations:

$$dAF(I,J)/dt = C\cdot V\cdot AF(I-1,J)(N + 1 - I - J)/N - C\cdot V\cdot AF(I,J)(N - I - J)/N + D\cdot AF(I+1,J)(I + 1) + f\cdot AF(I+1,J-1)(I + 1) - (f + D)AF(I,J)I \quad (3)$$

$$dV/dt = -C\cdot V \sum_{I+J=0}^{N-1} AF(I,J)(N - I - J)/N + D \sum_{I+J=1}^{N} AF(I,J)I \quad (4)$$

If deaggregation processes can be ignored ($D \ll f$; $D \ll CV_0$) and if there is little delay in the fusion of adhered virus particles, then adhesion is the rate-limiting step, and an appropriate analytical solution is readily obtained (Nir et al., 1986):

$$V(t) = V_0 \exp(-CG_0t) \quad (5)$$

Then the fraction $F(t)$ of fused virus particles is

$$[V_0 - V(t)]/V_0 = 1 - \exp(-CG_0t) \quad (6)$$

When $CG_0t \ll 1$

$$[V_0 - V(t)]/V_0 \approx CG_0t \quad (7)$$

The last equation implies a linear increase of the fraction of fused virus particles with time and with the initial concentration of erythrocyte ghosts. If fusion results in an infinite dilution of a certain fluorescent label (e.g., R_{18} molecules), then the expected increase in fluorescence intensity due to fusion should be proportional to the time and to the initial concentration of erythrocyte ghosts. As is explained in the Appendix, an expllcit account was taken of the dilution of R_{18} molecules as a result of fusion.

The actual calculations employed eq 1–4, but eq 5 was an adequate approximation in most cases. The criteria for the applicability of eq 5 are

$$D \ll f \qquad CV_0 \ll f \quad (8)$$

but at later stages eq 5 can still give a useful approximation when f is comparable to CV_0.

Results

Extent of Fusion. The extent of fusion between Sendai virus and erythrocyte ghosts can be deduced from the final levels of R_{18} fluorescence, which are shown in Table I for three cases, corresponding to three different virus and erythrocyte ghost batches. These results demonstrate that as the concentration of erythrocyte ghosts increases while the concentration of virus particles remains constant, the final levels of R_{18} fluorescence increase and approach 100%. An immediate conclusion arises that practially all of the virus particles are active, i.e., capable of fusion with erythrocyte ghosts.

The question remains, however, whether all virus particles have fused in cases where the final level of fluorescence increase is in the order of 20–50% or else is there an upper bound on the number of Sendai virus particles that can fuse with one erythrocyte ghost. The deduction from the results is that indeed such an upper bound exists, and furthermore, its determination from one case can yield reasonable predictions for the final levels of R_{18} fluorescence in other cases. Let I be the fractional increase in the final fluorescence intensity of R_{18} molecules due to their dilution as a result of fusion. I is given by

$$I = 1 - X \quad (9)$$

in which X is the relative surface concentration of R_{18} molecules, provided that their initial concentration is sufficiently low. Let us denote the surface areas of a single virus particle and an erythrocyte ghost by S_v and S_e, respectively, and let M be the average number of virus particles that have fused with a single cell. If all virus particles have fused, then

$$I = 1 - MS_v/(MS_v + S_e) = S_e/(S_e + MS_v) = 1/(1 + MS_v/S_e) \quad (10)$$

The ratio S_v/S_e can be roughly estimated from the dimensions of the particles, but we determined it directly from one of the experimental results, corresponding to 11.1 and 150 μg of viral and ghost protein/2 mL, since in this case it can be assumed that all virus particles have fused. By setting $I = 0.849$ (84.9%; cf. Table I) in eq 10, it follows that $S_e/(MS_v) = 5.6$. The number M is readily found as follows. A mass of 10 μg of ghost protein corresponds to 6.74 nmol of phospholipid. A ghost concentration of 150 μg/2 mL corresponds to a concentration of 50.5 μM erythrocyte phospholipid. The molar concentration of the above ghost particles amounts to $G_0 = 2.2 \times 10^{-13}$ M, which is obtained by using the value of 5.7×10^{-10} mg of protein/ghost particle. A concentration of 11.1 μg of protein of Sendai virus/2 mL corresponds to a phospholipid concentration of 1.53 μM (276 nmol of phospholipid/mg of protein). If the Sendai virus particle is approximated by a spherical vesicle of a diameter of 150 nm, then the above phospholipid concentration corresponds to $V_0 = 8 \times 10^{-12}$ M. Since it is assumed that in this case all virus particles have fused with the ghost particles, we find that $M = 37$, and with the result $S_e/(MS_v) = 5.6$, it turns out that $S_e/S_v = 207$. After S_e/S_v and M for this particular case have been determined, eq 10 can be employed to generate I values for other cases. For instance, for this virus concentration (11.1 μg of protein/2 mL) and 90 μg/2 mL ghost protein, $M = 62$. It turns out that by employing eq 10 the calculated I values agree well with the experimental values, provided that M values are below 100. When $M = 277$, the calculated I values are about 2 times larger than the experimental ones, and when $M = 460$, the disagreement is, of course, worse. However, all the experimental results of I values can be explained and predicted if we assume that M cannot exceed a certain value denoted by N. If the ratio between virus particles and ghosts is below N, then eq 10 is still valid. Otherwise, let p be the number of virus particles per ghost divided by N. If $p > 1$, eq 10 is modified to

$$I = 1/[p(1 + NS_v/S_e)] = 1/[p(1 + N/207)] \quad (11)$$

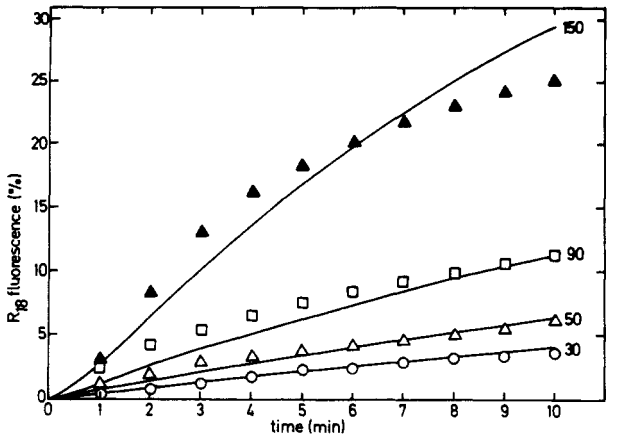

FIGURE 1: Kinetics of R_{18} fluorescence increase during fusion of labeled Sendai virus particles with erythrocyte ghosts at 37 °C and pH 7.4. Experimental values are given by data points, and calculated values are given by the drawn lines. The numbers 150, 90, 50, and 30 denote ghost concentrations in terms of micrograms of protein per 2 mL. The corresponding virus concentrations in terms of micrograms of protein per 2 mL are 11.1 (150), 16 (50), and 18.5 (90, 30). The rate constants employed in the respective calculations were as follows: $C = 3.5 \times 10^9$ M^{-1} s^{-1}, $f = 0.04$ s^{-1}, and $D = 0.0015$ s^{-1}; $C = 1.8 \times 10^9$ M^{-1} s^{-1}, $f = 0.07$ s^{-1}, and $D = 0.003$ s^{-1}; $C = 2.2 \times 10^9$ M^{-1} s^{-1}, $f = 0.04$ s^{-1}, and $D = 0.0015$ s^{-1}.

We have determined both p and N from the one experimental value $I = 0.239$ (23.9%), which was obtained in the case where the ghost and virus concentrations were 20 and 11.1 μg of protein/2 mL, respectively, i.e., $pN = 277$. From this value and eq 11, it follows that $p = 2.86$ and $N = 97$. The value of p (>1) was readily obtained for other cases by employing $N = 97$. Then, eq 11 and 10 were used to generate I values.

The calculated I values in Table I are fairly close to the experimental values. This is remarkable in view of the fact that three different virus batches were employed, and some size as well as functional variations may be expected.

It is relevant to note here that in the calculations in the previous paragraph we have used a viral concentration $V_0 = 8 \times 10^{-12}$ M, based on phospholipid. It is also possible to deduce this number from calculations based upon a viral molecular weight of 5×10^8 (Wolf et al., 1980) and assuming that 70% by weight is protein (Klenk & Choppin, 1969). Thus calculated, a value of 1.6×10^{-11} M for V_0 is obtained (11.1 μg of virus protein/2 mL), i.e., twice the value mentioned above. The use of this value for the virus concentration does not have an effect on the calculated values in Table I. It would only imply that when both values are taken into account, a lower limit for N of 97 ($V_0 = 8 \times 10^{-12}$ M) and an upper limit of 194 ($V_0 = 1.6 \times 10^{-11}$ M) can be determined, while the ratio of S_e/S_v would become 400.

In using eq 10 and 11, we have not accounted for a reduction in accessible surface area of the ghost by bound and unfused virus particles. The agreement between calculated and experimental I values can be improved by accounting for such reduction in accessible surface area, but this is a small effect as long as the number of virus particles bound per erythrocyte ghost does not exceed several hundreds.

We also examined the possibility that the fraction of active virus particles is $q < 1$. In this case, eq 10 is modified to

$$I = q/(1 + qMS_v/S_e) \qquad (12)$$

Again, we used the value $I = 0.849$ (last column in first row of Table I) but used $S_v/S_e = 1/2200$, which is obtained from the square of the ratio of virus and ghost diameters. This resulted in $q = 0.86$, i.e., 86% fusion. Then, the same procedure was followed and gave $N = 70$, i.e., similar to the previous value. The other calculated values of I were similar to the values presented in Table I, deviating by 1–2%. Thus, it should be emphasized that our results do not imply a significant reduction in the accessible surface area of the erythrocyte ghosts for dilution of R_{18} molecules.

Table II: Rate Constants Describing the Kinetics of Fusion of Sendai Virus[a] with Human Erythrocyte Ghosts at 37 °C and pH 7.4

adhesion rate constant, C (M^{-1} s^{-1})	fusion rate constant, f (s^{-1})	detachment rate constant, D (s^{-1})
3.5×10^9	0.04	0.0015
2.2×10^9	0.04	0.0015
1.8×10^9	0.07	0.003

[a] The parameters were obtained from an optimal fit to about 30 kinetic curves. The parameter C is relatively sharply defined, within 10% uncertainty, whereas the values of f and D are uncertain by about 50%. The three sets of parameters refer to three virus batches.

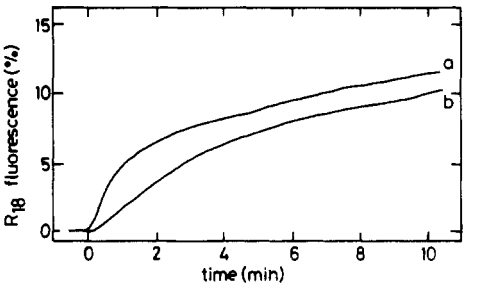

FIGURE 2: Effect of preattachment on virus–ghost fusion kinetics. A total of 16 μg of R_{18}-labeled viruses was incubated with 90 μg of ghosts at 4 °C in a final volume of 100 μL. After 15 min, prewarmed buffer was added, and fusion was monitored at 37 °C by following the increase of R_{18} fluorescence (curve a). Alternatively, the same amount of virus was directly injected into the fusion medium, containing the ghosts, i.e., without a low-temperature preincubation (curve b).

Kinetics of Fusion. An analysis of the kinetics of the increase in R_{18} fluorescence intensity provided information about the overall rate of fusion and about the rate constants. Figure 1 illustrates the initial kinetics of fluorescence intensity increase as a function of the erythrocyte ghost concentration for three virus concentrations that were obtained from three batches. The experimental results (data points) indicate that initially the rate of increase of fluorescence intensity (and hence fusion) is proportional to the ghost concentration, in accordance with eq 5–7. This increase in the rate of fusion is due to an increase in the rate of virus adhesion with the number of target sites (Hoekstra et al., 1985a).

In agreement with previous results of Lyles and Landsberger (1979), who monitored fusion by electron spin resonance, the rate of fusion is initially independent of the virus concentration. It should be pointed out that probe dilution depends on the ratio between the numbers (and surface areas) of virus particles and cells. This effect becomes more predominant at later stages, as we have pointed out earlier in presenting the results of final extents of fusion (see Table I). The rate constants of adhesion, C, fusion, f, and deadhesion, D, were determined by simulating the experimental data for a number of kinetic curves. Fair predictions could be made regarding the kinetics of all other cases. For brevity, we present in Figure 1 just four curves out of a total of 30 cases. The values of the rate constant are given in Table II. In determining the parameters, we were also guided by results of preincubation experiments at 4 °C. Preincubation of virus particles and erythrocyte ghosts at 4 °C results in their adherence to the ghosts but does not yield fusion (Wolf et al., 1980; Hoekstra et al., 1985a) until the sample is brought to a higher temperature, such as 37 °C.

Figure 2 illustrates that preincubation in the cold enhanced the initial rate of fusion due to the fact that a majority of the virus particles were bound at the onset of the temperature increase. It may be noted that several minutes after the onset of the incubation at 37 °C the levels of fluorescence intensity are almost independent of the preincubation period in the cold. At 4 °C, particle detachment could be ignored, whereas at 37 °C virus detachment occurred at a comparable rate to fusion (D. Hoekstra, unpublished results). The preincubation experiments and the amount of subsequent virus detachment provided a rough estimate and test for the values of the parameters f and D, since under those conditions the initial rate of fusion and dissociation are less affected by the value of the rate constant of adhesion, C.

Discussion

In this study a mass action model has been applied, for the first time, to the analysis of the results of fusion between two biological membranes, i.e., the membrane of an erythrocyte and that of a Sendai virus. The model views the overall fusion reaction as a sequence of a second-order process of adhesion of the virus particles to the cells followed by the first-order fusion reaction that amounts to local destabilization and subsequent merging of the apposed membranes. The kinetics of this fusion process, as monitored by the fluorescence increase, occurring upon randomization of viral and target membrane components (Hoekstra et al., 1984), could be well simulated and predicted by the model. It has been well documented (Hoekstra et al., 1984, 1985a) that the dilution of R_{18} molecules arises from fusion rather than from a transfer of individual molecules, mediated either by a transfer through the aqueous phase or by a collision–contact mechanism. It can be added that the observed proportional increase of the initial rate of fluorescence increase as a function of the ghost concentration is also compatible with a fusion mechanism rather than with an exchange mechanism. Furthermore, as we have pointed out, the final levels of R_{18} fluorescence can be entirely explained by setting a limit of 100–200 to the number fo Sendai virus particles fusing with one cell, and no such limit can be envisaged for a mechanism involving molecular exchange or transfer.

Independent of the kinetic model and the values of the rate constants, valuable information can also be obtained from the analysis of the final levels of fluorescence increase, i.e., after incubation times exceeding 20 h. The analysis revealed that almost all Sendai virus particles are active, i.e., are capable of fusing with erythrocyte ghosts at 37 °C, pH 7.4. However, while the number of virus particles bound per cell can exceed 1000 (Wolf et al., 1980; D. Hoekstra and K. Klappe, unpublished results), the number of particles that actually fuse with a single cell is just in the order of 100. This result illustrates the importance of keeping the ratio of virus particles to ghosts below a certain limit if the primary aim is to achieve virus–target membrane fusion with the highest fusion efficiency possible, relative to the total viral dose added. Vice versa, if the focus is on particle binding, then a large ratio such as 1000 particles per cell is desirable, since in this case the contribution of fusion to particle association with cells is relatively small.

A most interesting and intriguing outcome of the analysis reported here is the finding that the number of particles fusing with a single erythrocyte ghost is limited to about 100. This may reflect that a limited number of receptor sites exists on the cell surface at which the binding of the virus will eventually lead to fusion. This interpretation would be consistent with previous observations reported by Richardson and Choppin (1983) that oligopeptides, resembling the amino acid sequence of the N-terminal region of the F_1 polypeptide, specifically inhibit the fusion of paramyxoviruses with the plasma membrane of the host cell. The N-terminus of the F_1 subunit is formed during a posttranslational stage as a result of a proteolytic cleavage of the (inactive) F protein by a host cell enzyme (Scheid & Choppin, 1981). It contains a sequence of amino acids that is unusually hydrophobic (Hsu et al., 1981), and this segment is thought to be involved in the fusion process per se by interacting directly with the target membrane (Choppin et al., 1981; White et al., 1983). Although both the results presented by Richardson and Choppin (1983) and those reported in the present work could be taken to indicate that receptor sites for the F_1 polypeptide exist on cell membranes, it is also possible that the presence of spikes from fused viruses inhibits the fusion of additional ones. In this context, we note that in studies on the fusion between influenza virus and liposomes consisting of cardiolipin (Stegmann et al., 1985; Nir et al., 1986), it was found that the fusion products may consist of several liposomes, but they include just a single virus. However, the surface area of a single liposome is about the same as that of an influenza virus, whereas at a ratio of 100 Sendai virus particles per ghost the average area is 20 times larger than that of the combined surface areas of the fused virus particles. On the other hand, the analysis of the kinetics (Figure 1) does not exclude the possibility that there is a slight tendency of reduction in the rate constants of fusion and/or adhesion as the reaction proceeds. In addition, the potential fusion sites (see above) may not be randomly distributed in the plane of the bilayer, and therefore, the rate of viral protein diffusion (Bächi et al., 1977; Loyter & Volsky, 1982) from these "fusion areas" may additionally affect the fusion ability of viral particles that are about to fuse.

Our kinetic analysis provides a quantitative description of the distribution of adhesion-fusion products. Table III gives the relative concentrations of a few representative cases at three times, t = 1, 2, and 10 min. At t = 1 min, most of the virus particles that are associated with the cells are accounted for by products containing up to five virus particles, and the percent of free ghosts is 25. After 10 min, the distribution is predominantly accounted for by products containing 10 or more particles; i.e., there are, essentially, no free ghosts left. Furthermore, despite the relatively small magnitude of the

Table III: Distribution of Adhesion-Fusion Products[a]

virus–ghost adhesion-fusion products	fraction of initial ghost concn at time (min)		
	1	2	10
AF(0,0)	0.25	0.07	4×10^{-6}
AF(1,0)	0.11	0.03	2×10^{-6}
AF(0,1)	0.24	0.16	6×10^{-5}
AF(1,1)	0.10	0.07	2×10^{-5}
AF(2,0)	0.02	0.006	3×10^{-7}
AF(0,2)	0.11	0.18	4×10^{-4}
AF(5,0)	3×10^{-4}	8×10^{-6}	2×10^{-10}
AF(0,5)	1.4×10^{-3}	0.03	0.013
AF(5,5)	10^{-7}	3×10^{-6}	4×10^{-7}
AF(10,0)	8×10^{-12}	3×10^{-12}	3×10^{-17}
AF(0,10)	2×10^{-8}	4×10^{-5}	0.097
% virus associated with cells	3.1	4.8	20.9
% fluorescence increase	1.7	4.1	19.2

[a] AF(I,J) is an adhesion-fusion product describing a ghost particle whose membrane includes I adhered and J fused virus particles. The numbers in the table refer to concentrations of these constructs relative to the initial ghost concentration. AF(0,0) is the relative concentration of free ghost. These calculated values employed virus and ghosts concentrations of 16 and 150 μg of protein/2 mL, respectively. The rate constants used were $C = 1.8 \times 10^9$ M^{-1} s^{-1}, $f = 0.07$ s^{-1}, and $D = 0.003$ s^{-1}.

fusion rate constants (vide infra), fusion can be considered fast relative to adhesion except at the earliest times up to t = 1 min, where the corresponding rates are comparable. At t = 2 min, AF(0,1) is 5 times larger than AF(1,0), and AF(0,5) (the concentration of ghost particles that incorporated five virus particles by fusion) is 4000 times larger than AF(5,0). After 10 min, the fraction of nonfused virus particles of those associated with cells is very small. We note, however, that the values in Table III were generated by employing the largest f value in the range given in Table II.

Initially, the dilution of R_{18} molecules due to fusion of virus particles is expected to be practically infinite, whereas as fusion proceeds the percent of fluorescence increase may be smaller than the percent of fused virus particles. At 10 min, i.e., when the percent fluorescence increase is close to 20, this value is close to the percent of fused virus particles. Hence, as long as the ratio between ghost and virus particles is optimal (e.g., 150/16 μg of protein), the percent of fluorescence increase yields an immediate estimate for percent of virus fusion. In Table III, about 20% of the virus particles became associated with the cells after 10 min. It may be noted that a preincubation for several minutes at 4 °C is expected to result in an almost complete binding of virus particles (cf. Figure 2), because the concentration of particles in the preincubation experiments is 20 times larger than that during the fusion experiments at 37 °C, while the dissociation rate constant is very small at 4 °C. This was obtained by our calculations and confirmed by direct measurements (D. Hoekstra and K. Klappe, unpublished results).

The values found for the rate constant of adhesion C = (1.9–3.5) × 10^9 M^{-1} s^{-1} are close to the values in diffusion-controlled processes (Smoluchowski, 1917). In comparison, C values deduced from the fusion kinetics of infuenza virus with cardiolipin vesicles at pH 5 are somewhat lower, (0.5–1) × 10^9 M^{-1} s^{-1}, yet even these values are large relative to the values found for vesicle–vesicle aggregation. We attribute the large C values found for these two viruses to the existence of spikes on their envelopes, which amounts to local areas of a small radius of curvature, and hence a small potential barrier for close approach (Nir et al., 1980a,b). The binding of the virus to receptors on the surface of the ghost is expected to further promote the rate of adhesion.

Table II indicates that the values found for the rate constants of fusion are 0.04–0.07 s^{-1}, whereas the values found for influenza virus fusing with cardiolipin vesicles were 0.9–1.7 s^{-1} at pH 5 and 0.25 s^{-1} at pH 6 (Nir et al., 1986). In comparison, f values found for the fusion of large phosphatidylserine vesicles induced to fuse by several millimolar of Ca^{2+} were in the range of 0.1–1 s^{-1} (Nir et al., 1982, 1983; Bentz et al., 1983a,b, 1985), and values found (Wilschut et al., 1985) for the fusion of large vesicles composed of equimolar mixtures of cardiolipin and phosphatidylcholine (10 mM Ca^{2+}) were also in this range. Thus, it appears that compared with the above fusion systems the destabilization and rearrangement of the fusing membranes of Sendai virus and erythrocyte ghost is a relatively slow process. It may be noted that Lyles and Landsberger (1979) reported values of $t_{1/2}$ of about 10 min for the overall fusion reaction, whereas our analysis distinguishes between adhesion and the actual fusion event. The small rate constant of fusion does not cause a serious delay in the overall reaction (see Table III). In a hypothetical situation where all virus particles adhere to the ghosts and no dissociation occurs, the relative number of fused virus particles is given by $1 - \exp(ft)$, where t is the time from the onset of the fusion reaction. When $ft \ll 1$, the above expression reduces to ft. Thus, with f = 0.02 s^{-1}, it will take 10 s until 20% of the adhered particles fuse. The actual process is somewhat slower because of a certain degree of dissociation.

The value found for the dissociation or detachment rate constant D is 1 order of magnitude below that of f, and thus, it does not substantially affect the results shown in Figure 1. We have explicitly included the consideration of dissociation processes in the calculations mainly because of the realization that there are conditions where dissociation may play an important role. For instance, upon transference of a suspension preincubated at 4 °C to a medium at 37 °C (D. Hoekstra and K. Klappe, unpublished results), about one-third of the cell-associated virus particles dissociate from the ghosts within a few minutes, while the fusion reaction, resulting in irreversible association of viral material with the ghosts, proceeds.

Our conceptual picture of the aggregation or adhesion step is that of a dynamical process where particles adhere and dissociate continuously (Nir et al., 1980b, 1983; Bentz & Nir, 1981a,b; Bentz et al., 1985). It appears that such a picture also applies to virus–target membrane interaction. The simultaneous occurrence of membrane fusion further adds to the complexity of the overall interaction process. The application of the mass action model presented here provides a unique opportunity, however, to unravel these distinct steps and analyze them kinetically. As demonstrated, this opens new possibilities to define more accurately the various parameters affecting the fusion process, i.e., aggregation, detachment, or fusion per se, and, hence, to obtain a better insight into the mechanism of fusion between biological membranes.

ACKNOWLEDGMENTS

S.N. acknowledges useful discussions with Prof. A. Loyter. We gratefully appreciate the expert secretarial assistance of Rinske Kuperus.

APPENDIX

Numerical Solutions of Equations for the Kinetics of Fusion. Equations 1–4 describe the kinetics of adhesion, deadhesion, and fusion of virus particles and erythrocyte ghosts, ignoring (see Theory) aggregation and fusion between ghost particles. The numerical solutions were obtained by means of a Taylor expansion, which included four terms. Let the function y stand for any of the functions AF(I,J) or V. The Taylor expansion is

$$y(t+h) = y(t) + hy'(t) + h^2y''(t)/2 + h^3y'''(t)/6 \qquad \text{(A1)}$$

in which h is the time increment. At t = 0, $V = V_0$; AF(I,J) = 0 for I and $J \geq 1$ and AF(0,0) = G_0. Equations 3 and 4 provide the first derivatives, and the second and third derivatives are successively obtained. After having determined the derivatives at time t, eq A1 provides the functions V and AF(I,J) at time $t + h$. The increment h is chosen to ensure the desired accuracy. One test for accuracy was the mass conservation relations, eq 1 and 2. The fact that the weighted sums obtained by taking the derivatives of these equations should vanish was employed to provide another sensitive test on accuracy.

Calculation of Increase in Fluorescence Intensity. Dilution of R_{18} molecules upon the fusion of virus particles with erythrocyte ghosts results in an increase of their fluorescence (see eq 9). The fractional increase in fluorescence intensity, I, is given by

$$I = \sum_{I+J=1}^{N} J\cdot\mathrm{AF}(I,J)\mathrm{DL}(J)/V_0 \qquad \text{(A2)}$$

The factor DL(J) reflects the degree of dilution of R_{18} molecules on the surface of an erythrocyte ghost, which incorporated by fusion J virus particles. Initially, the dilution is almost complete, and the DL factors are close to unity. The factor DL(J) is given by eq A3 in which S_v/S_e is the ratio between the areas of a virus particle and an erythrocyte ghost, as described under Results.

$$DL(J) = 1 - X = 1 - JS_v/(JS_v + S_e) = 1/(1 + JS_v/S_e) \quad (A3)$$

References

Bächi, T., Deas, J. E., & Howe, C. (1977) *Cell Surf. Rev. 2*, 83–128.

Bentz, J., & Nir, S. (1981a) *Proc. Natl. Acad. Sci. U.S.A. 78*, 1634–1637.

Bentz, J., & Nir, S. (1981b) *J. Chem. Soc., Faraday Trans. 1 77*, 1249–1275.

Bentz, J., Nir, S., & Wilschut, J. (1983a) *Colloids Surf. 6*, 333–363.

Bentz, J., Düzgünes, N., & Nir, S. (1983b) *Biochemistry 22*, 3320–3330.

Bentz, J., Düzgünes, N., & Nir, S. (1985) *Biochemistry 24*, 1064–1072.

Choppin, P. W., & Scheid, A. (1980) *Rev. Infect. Dis. 2*, 40–61.

Choppin, P. W., Richardson, C. D., Merz, D. C., Hall, W. W., & Scheid, A. (1981) *J. Infect. Dis. 143*, 352–363.

Cohen, C. M., & Solomon, A. K. (1976) *J. Membr. Biol. 29*, 345–372.

Harmsen, M. C., Wilschut, J., Scherphof, G., Hulstaert, C., & Hoekstra, D. (1985) *Eur. J. Biochem. 149*, 591–599.

Haywood, A. M. (1974) *J. Mol. Biol. 83*, 427–436.

Hoekstra, D., De Boer, T., Klappe, K., & Wilschut, J. (1984) *Biochemistry 23*, 5675–5681.

Hoekstra, D., Klappe, K., De Boer, T., & Wilschut, J. (1985a) *Biochemistry 24*, 4739–4745.

Hoekstra, D., Wilschut, J., & Scherphof, G. (1985b) *Eur. J. Biochem. 146*, 131–140.

Holmgren, J., Svennerholm, L., Elwing, H., Fredman, P., & Strunnegard, O. (1980) *Proc. Natl. Acad. Sci. U.S.A. 77*, 1947–1950.

Hosaka, Y., & Shimizu, K. (1977) *Cell Surf. Rev. 2*, 129–155.

Hsu, M.-C., Scheid, A., & Choppin, P. W. (1981) *J. Biol. Chem. 256*, 3557–3563.

Klenk, H.-D., & Choppin, P. W. (1969) *Virology 37*, 155–157.

Lee, P. M., Cherry, R. J., & Bächi, T. (1983) *Virology 128*, 65–76.

Lenard, J., & Miller, D. K. (1983) in *Receptor-Mediated Endocytosis and Processing* (Cuatrecasas, P., & Roth, T., Eds.) pp 121–138, Chapman and Hall, London.

Loyter, A., & Volsky, D. J. (1982) *Cell Surf. Rev. 8*, 215–266.

Lyles, D. S., & Landsberger, F. R. (1979) *Biochemistry 18*, 5088–5095.

Nir, S., Bentz, J., & Wilschut, J. (1980a) *Biochemistry 19*, 6030–6036.

Nir, S., Bentz, J., & Portis, A. (1980b) *Adv. Chem. Ser. No. 188*, 75–106.

Nir, S., Wilschut, J., & Bentz, J. (1982) *Biochim. Biophys. Acta 688*, 275–278.

Nir, S., Bentz, J., Wilschut, J., & Düzgünes, N. (1983) *Prog. Surf. Sci. 13*, 1–124.

Nir, S., Stegmann, T., & Wilschut, J. (1986) *Biochemistry 25*, 257–266.

Poste, G., & Pasternak, C. A. (1978) *Cell Surf. Rev. 5*, 305–367.

Richardson, C. D., & Choppin, P. W. (1983) *Virology 131*, 518–532.

Smoluchowksi, M. (1917) *Z. Phys. Chem., Abt. A 92*, 129–168.

Steck, T. L., & Kant, J. A. (1974) *Methods Enzymol. 31*, 172–180.

Stegmann, T., Hoekstra, D., Scherphof, G., & Wilschut, J. (1985) *Biochemistry 24*, 3107–3113.

Umeda, M., Nojima, S., & Inoue, K. (1983) *J. Biochem. (Tokyo) 94*, 1955–1966.

Umeda, M., Nojima, S., & Inoue, K. (1984) *Virology 133*, 172–183.

White, J., Kielian, M., & Helenius, A. (1983) *Q. Rev. Biophys. 16*, 151–195.

Wilschut, J., & Hoekstra, D. (1984) *Trends Biochem. Sci. (Pers. Ed.) 9*, 479–483.

Wilschut, J., Nir, S., Scholma, J., & Hoekstra, D. (1985) *Biochemistry 24*, 4630–4636.

Wolf, D., Kahan, I., Nir, S., & Loyter, A. (1980) *Exp. Cell Res. 130*, 361–369.